

High-pressure vibrational spectroscopy of sulfur dioxide

Yang Song,^{a)} Zhenxian Liu, Ho-kwang Mao, and Russell J. Hemley
*Geophysical Laboratory, Carnegie Institution of Washington, 5251 Broad Branch Road, NW,
 Washington, DC 20015*

Dudley R. Herschbach
*Department of Chemistry and Chemical Biology, Harvard University, 12 Oxford Road, Cambridge,
 Massachusetts 02138*

(Received 16 November 2004; accepted 8 February 2005; published online 5 May 2005)

Solid sulfur dioxide was investigated by vibrational spectroscopy over a broad pressure and temperature range, extending to 32.5 GPa at 75–300 K in diamond anvil cells. Synchrotron infrared spectra provided the first measurements of the pressure dependence of the lattice modes in the far-IR region. Below 17.5 GPa, two fundamentals exhibit splittings enhanced by pressure. The asymmetric stretching mode of SO₂ exhibits a remarkable pressure-induced softening. The observations are consistent with the ambient pressure Raman measurements indicating that SO₂ crystallizes in an acentric cell, but are inconsistent with a previously proposed interpretation that the structure of the high-pressure phase consists of (SO₂)₃ clusters. Dramatic changes in the Raman spectra are found above 17.5 GPa at room temperature. These indicate major changes in structure and possible formation of SO₂ clustering with an enlarged unit cell. The behavior at low temperature differs from that at room temperature. These findings provide constraints on the phase diagram of sulfur dioxide. © 2005 American Institute of Physics. [DOI: 10.1063/1.1883405]

I. INTRODUCTION

Sulfur dioxide is an important molecule in atmospheric, geological, and chemical sciences. Because SO₂ can be either a Lewis acid or base, either oxidant or reductant due to its unique molecular and electronic configuration, it is highly reactive and plays a role in extensive chemical applications.¹ Its vibrational, rotational, and electronic structures have been widely investigated both experimentally and theoretically in gas phase (i.e., ambient conditions).^{2–9} The isolated molecule has a C_{2v} symmetry and its three fundamental vibrational modes, i.e., ν_1 (A_1 , S=O symmetric stretch), ν_2 (A_1 O=S=O deformation), and ν_3 (B_1 , S=O asymmetric stretch), are all both infrared and Raman active. Sulfur dioxide condenses at 263 K and freezes at 198 K. The crystal structure of SO₂ has been determined by Post *et al.*¹⁰ using single-crystal x-ray diffraction at 143 K. Solid SO₂ has an orthorhombic structure with four molecules per unit cell with space group Aba (C_{2v}^{17}) and cell parameters $a=6.07$ Å, $b=5.94$ Å, and $c=6.14$ Å, yielding a cell volume of 221 Å³ and density of 1.92 g/cm⁻³. The S=O bond length is 1.43 Å and the O=S=O angle is 119°. Anderson and Campbell⁶ reported high-resolution infrared and Raman spectra of crystalline SO₂ at 20 K. Numerous spectral features associated with SO₂ molecular and lattice vibrations were observed and assigned. Later Brooker⁷ conducted a more detailed investigation of the structure of solid sulfur dioxide by Raman spectroscopy at 77 K. This study further confirmed the orthorhombic structure consistent with the acentric C_{2v}^{17} space group. In the analysis of the spectral pro-

file and assignment, the correlation field and isotopic effects associated with molecular SO₂ were taken into account.

These optical studies as well as the x-ray diffraction data elucidated fundamental properties of sulfur dioxide at ambient pressure and low temperatures. However, unlike other fundamental molecular species such as CO₂, H₂O, etc., whose high P - T structures have been explored in detail in recent years,^{11,12} high-pressure data for sulfur dioxide have been lacking. Raman spectroscopy of condensed phase SO₂ was studied by Swanson *et al.*¹³ more than two decades ago, but only up to 7.5 GPa. Even in that narrow pressure range, evidence was found for three solid phases. In addition to the known orthorhombic phase (designated as solid I) at ambient pressure, compression of liquid SO₂ at room temperature and 0.3 GPa results in the formation of colorless solid phase II; further compression to 2.5 GPa gives another yellowish solid phase III. These two new phases have entirely different structures than solid phase I as evidenced by different patterns of the ν_1 and ν_2 fundamentals in the Raman spectra. In phase II all three fundamentals appear as broad peaks and no well-defined lattice modes were observed in the low-energy region, indicating molecular disorder. The transition from phase II to phase III transition seems to be a sharp first-order transition since in phase III both the ν_1 and ν_2 bands sharpen and split into doublets or triplets. The structure of phase III is not clear, but it has been proposed that this phase is characterized by aggregation of the SO₂ molecules, e.g., trimetric (SO₂)₃. This phase was also found to be sensitive to both blue and green laser radiation.

However, the findings of Swanson *et al.*¹³ were inconsistent with the ambient pressure structure reported earlier.^{7,10} In particular, based on the complex Raman fea-

^{a)}Author to whom correspondence should be addressed. Electronic mail: y.song@gl.ciw.edu

tures observed both in phase I and phase III, it was suggested¹³ that solid SO₂ crystallized in a centric space group, instead of the previously reported C_{2v}^{17} acentric space group.^{7,10} In interpreting the splittings of the fundamentals, they ignored factor group effects arising from trimerization of monomeric SO₂ were not considered. Brooker⁷ later pointed out that this analysis also ignored isotopic effect and longitudinal-optical modes associated with SO₂ vibrations. Therefore, the high-pressure structure of SO₂ remains unclear.

Recent advances in diamond-anvil cell (DAC) techniques have opened new avenues for exploring the behavior of simple molecular systems over a wide P - T range^{11,12} using a variety of spectroscopic and diffraction measurements.^{14–16} We take advantage of these techniques to study the vibrational spectra of SO₂ up to 32.7 GPa and from room temperature down to 75 K. New pressure-induced phases are identified from Raman and IR measurements. The fundamental bands exhibit peculiar pressure-induced behavior, including enhanced splittings and mode softening, not observed in the previous low or ambient pressure studies. At low temperature and high pressure, we obtained high-quality Raman spectra with well-resolved lattice modes. We also report the first IR spectra of pressurized SO₂, including far-IR spectra obtained with a synchrotron-radiation source. These results enable us to reinterpret the high-pressure structures of solid sulfur dioxide.

II. EXPERIMENT

Pure sulfur dioxide (99%) was purchased from Aldrich and used without further purification. Loading was done by precooling a DAC in liquid nitrogen. The melting point for SO₂ is -75 °C so gaseous SO₂ solidifies on the cooled rhenium gasket of the cell in a liquid-nitrogen bath. The cells were then sealed and the solid SO₂ pressurized before warming to room temperature. A ruby chip was inserted for pressure measurement. The pressure was determined from the pressure shift of the R_1 ruby fluorescence line with an accuracy of ± 0.05 GPa under quasihydrostatic conditions.¹⁷ For Raman studies, both the 488.0- and 514.5-nm lines of an Ar⁺ laser (Coherent Innova 90) were used as the excitation source, with an average power of 0.1 W or less. A 460-mm focal length $f/5.3$ imaging spectrograph (ISA HR460) equipped with a 1800-grooves/mm grating with a resolution of ± 0.5 cm⁻¹ was used. Calibration of the Raman spectrum with Ne lines provided an accuracy of ± 1 cm⁻¹. A custom-built optical cryostat was used for the low-temperature Raman measurements; the temperature range from 80 to 300 K was explored using liquid nitrogen as the cryogen.

Infrared-absorption spectra were measured at beamline U2A of the National Synchrotron Light Source (NSLS), Brookhaven National Laboratory (BNL). The optical layout has been described in detail elsewhere.¹⁸ Briefly, the synchrotron light is collected from a source in a 40×40 -mrad solid angle and collimated to a 1.5-in.-diameter beam before entering a Bruker IFS 66v vacuum Fourier transform infrared (FTIR) spectrometer. The spectrometer was equipped with a number of beam splitters and detectors including a

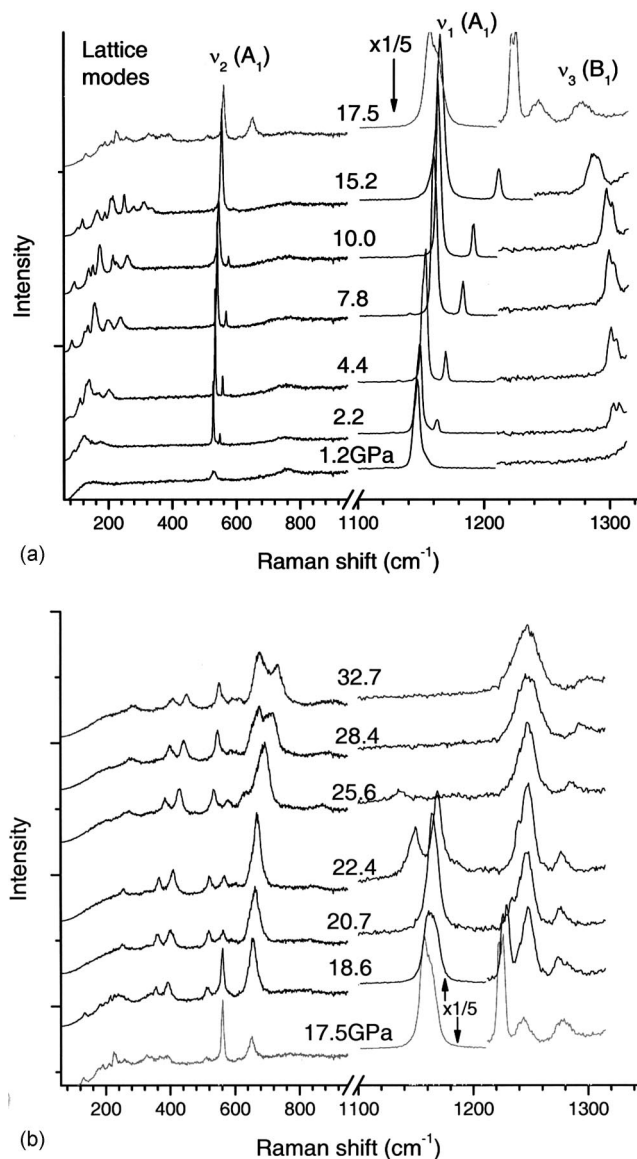


FIG. 1. Raman spectra of solid SO₂ in the pressure range of (a) 1.2–17.5 GPa and (b) 17.5–32.7 GPa collected at room temperature. Due to the high intensity of the ν_1 mode, the spectra are scaled by 1/5 between 1100 and 1200 cm⁻¹ for pressures between 1.2 and 18.6 GPa. As Raman scattering by the diamond anvils becomes dominant near 1340 cm⁻¹, the spectra are truncated at that frequency.

silicon bolometer and mercury cadmium telluride (MCT). In addition, a grating spectrograph with a charge-coupled device (CCD) array detector was used in the visible, giving complete coverage of the spectral range from 50 to 20 000 cm⁻¹. The resolution used in the present study was 4 cm⁻¹.

III. RESULTS

A. Room-temperature Raman spectra

Figure 1 shows Raman spectra of molecular SO₂ at room temperature on compression from 1.2 to 32.7 GPa. Typically each spectrum consists of four Raman-active regions, i.e., the lattice region, ν_2 (A_1 O=S=O deformation) region at

530–570 cm⁻¹, ν_1 (A_1 , S=O symmetric stretch) at about 1146–1168 cm⁻¹, and ν_3 (B_1 , S=O asymmetric stretch) at 1280–1310 cm⁻¹.

At 1.2 GPa [Fig. 1(a)], no lattice modes are seen and the ν_2 mode is a fairly broad and weak singlet; these features are consistent with disordered structures identified previously as solid phase II.¹³ Due to the strong first-order Raman scattering of the diamond anvils around 1340 cm⁻¹, the ν_3 mode of SO₂ is buried under its front tail. Upon slight compression to 2.2 GPa, a feature emerges in the low-frequency region and both ν_1 and ν_2 modes split into doublets; at the same time, the ν_3 band becomes visible at 1305 cm⁻¹. These striking changes indicate the phase transition at 2.2 GPa from phase II to phase III. Further compression to 15.2 GPa results in the development of more sharply resolved lattice modes and pressure-induced frequency shifts. At 15.2 GPa seven lattice modes are clearly resolved. Starting from 2.2 GPa, the ν_1 mode begins to split and the splitting increases markedly with pressure, from 14 cm⁻¹ at 2.2 GPa to 68 cm⁻¹ at 15.2 GPa. On compression, the frequencies of all bands shift to higher values, except for the ν_3 asymmetric stretching band. Notably, this mode shifts to lower frequency on compression at a rate of -1.9 cm⁻¹/GPa. This soft-mode behavior suggests that a phase transition will occur on further compression.¹⁹

The Raman spectrum of SO₂ at higher pressures is shown in Fig. 1(b). Striking features are observed for all the Raman-active modes, starting at 17.5 GPa: (1) The lattice modes seem to smear out; (2) a new mode, instead of high-frequency component of the ν_2 doublet, occurs at 653 cm⁻¹; (3) the doublet of the ν_1 mode changed to singlet with a significantly broadened profile and shift to red; and (4) a new band with two components at 1224 and 1244 cm⁻¹ appears below the ν_3 mode. These changes not only indicate a different lattice structure but also suggest major changes in the molecular structure. At 18.6 GPa, this transition continues to develop as evidenced by the growth of the new modes around 653, 1224, and 1244 cm⁻¹. These modes are fully developed at 20.7 GPa except that the latter two modes have merged into a singlet. At the next pressure 22.4 GPa, the ν_1 mode has split again as below 17.5 GPa, but with a much smaller separation of 19 cm⁻¹ as compared to 47 cm⁻¹ at 15.2 GPa. This band completely disappeared when the pressure was further increased to 28.4 GPa. From that pressure to 32.7 GPa, the highest pressure of the Raman measurements, the only significant new feature is the splitting of a 653-cm⁻¹ band into a doublet.

These pressure-induced changes are summarized in Fig. 2, which plots the Raman frequencies versus pressure. The external modes are omitted; these will be discussed below with the low-temperature measurements. Below 17.5 GPa, both the ν_1 and ν_2 doublets exhibit a smooth evolution on compression at average rates of 1.9 and 3.3 cm⁻¹/GPa for the ν_2 doublet and 1.2 and 3.8 cm⁻¹/GPa for the ν_1 . The significantly different pressure dependence of the two components of the doublets causes the splitting to increase remarkably upon compression. In contrast to ν_1 and ν_2 , as mentioned above, the ν_3 band exhibits a negative shift of -1.9 cm⁻¹/GPa. In addition to the smooth evolution of these

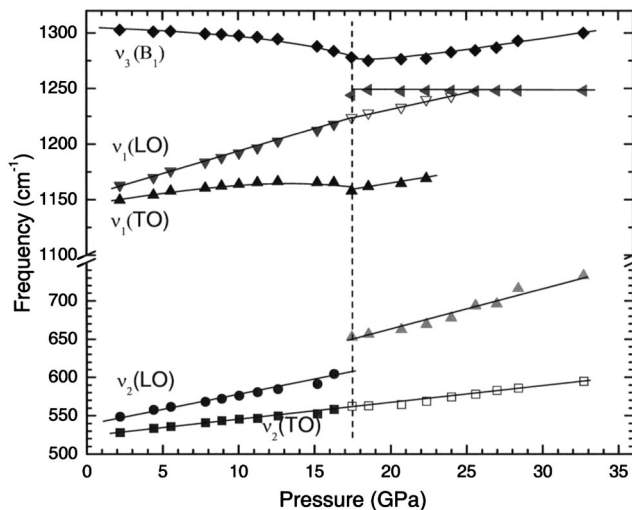


FIG. 2. Pressure dependence of Raman shifts of the three fundamental vibrational modes of solid SO₂. Different symbols denote different origins associated with each vibrational mode. The open symbols, although reside on the same line of the prior solid ones, are assigned as different modes (see text). The vertical dashed line represents a phase boundary, above which new phases appear as indicated by new Raman bands.

three vibrational modes, the lattice region exhibits similar patterns at all pressures below 17.5 GPa. We conclude that between 2.2 and 17.5 GPa, sulfur dioxide crystallizes in an ordered structure, extending the range of the previously identified phase III from 7.5 to 17.5 GPa.¹³

B. Low-temperature Raman spectra

In order to compare with the previous low-temperature optical measurements, we also obtained Raman spectra of solid SO₂ *in situ* at high pressures and low temperature. The previous high-pressure measurements on SO₂ were only conducted at room temperature.¹³ Figure 3 shows the Raman spectra of SO₂ we obtained at seven pressures from

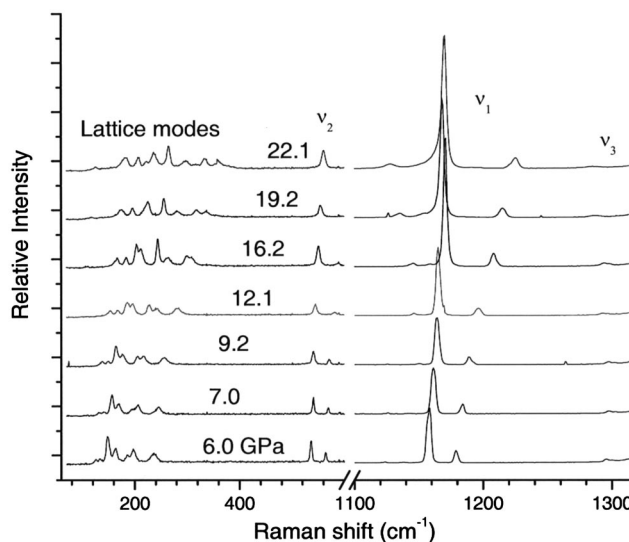


FIG. 3. Raman spectra of solid SO₂ in the pressure range between 6.0 and 22.1 GPa collected at 75 K. As Raman scattering by the diamond anvils becomes dominant at about 1340 cm⁻¹, the spectra are truncated at that frequency.

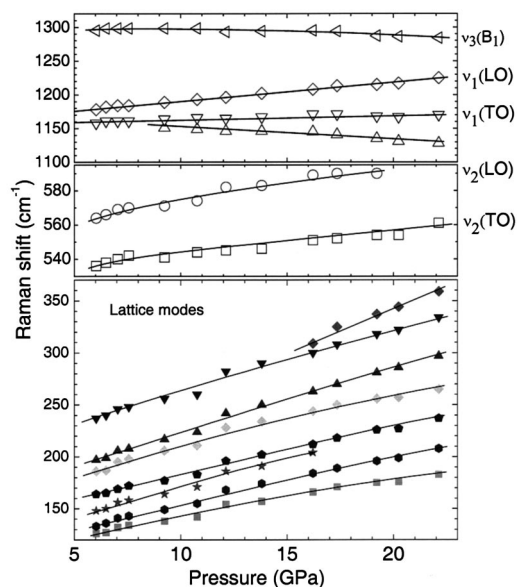


FIG. 4. Pressure dependence of the Raman modes of solid SO_2 .

6.0 to 22.1 GPa and 75 K. As in the room-temperature measurements, these display four Raman-active regions, i.e., the lattice region and the internal modes ν_2 , ν_1 , and ν_3 vibrational mode regions but all the peaks are sharper in the low-temperature spectra. Figure 4 shows the pressure-induced shifts for lattice modes as well as the internal modes.

In contrast to the behavior observed at room temperature, the Raman profiles exhibit no qualitative changes at low temperature over the entire range from 6.0 to 22.1 GPa. Specifically, the ν_2 (A_1 O=S=O deformation) bands occur as a doublet at all pressures, although as the pressure increases, the high-frequency component fades and nearly disappears at 20.2 and 22.1 GPa. The separation between the doublets remains fairly constant on compression (Fig. 4, middle panel) in contrast to the pressure-dependent splitting of the two components observed at room temperature (Fig. 2).

The most prominent pressure-induced behavior is observed for the ν_1 symmetric stretching mode of SO_2 . Over the whole pressure range, the low-frequency component of the doublet exhibits no appreciable pressure-induced frequency shift and remains near 1165 cm^{-1} . The high-frequency component, however, shifts steadily to higher values with pressure. Unlike the room-temperature spectra, where a new band is observed on the high-frequency side of the ν_1 mode starting from 17.5 GPa, the corresponding band is not observed up to 22.1 GPa. Instead a new peak on the low-frequency side ($\sim 1151\text{ cm}^{-1}$) starts to develop (Fig. 3), starting from 9.2 GPa. With the increasing pressure, the intensity of this peak grows systematically and its frequency of this new peak shifts downwards. The frequency of ν_3 at 75 K remains more or less constant at 1295 cm^{-1} , in contrast to ν_3 at room temperature, which decreases with pressure up to 17.5 GPa then increases. These observations indicate the existence of phase transitions but the transition pressures appear to be different than at room temperature.

The well-resolved lattice modes at low temperature help to identify possible phase transitions.¹⁴ The Raman dependence of these lattice frequencies provides further evidence

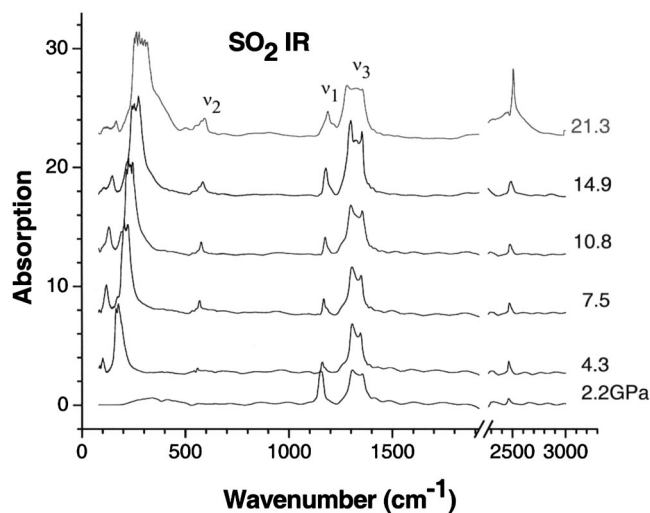


FIG. 5. Synchrotron IR spectra of solid SO_2 of $100\text{--}2500\text{ cm}^{-1}$ measured at room temperature for six pressures. The absorbance has been normalized with respect to the beam current of the synchrotron light source. The region of $1900\text{--}2200\text{ cm}^{-1}$ is omitted because of interfering absorption from the Type-II diamonds used as anvils. The assignments of the three fundamental modes are shown above the corresponding IR bands.

for the phase transitions indicated by the internal vibrational modes. As shown in Fig. 4, at most pressures there are seven Raman bands corresponding to librations and rotations in the frequency range of $100\text{--}350\text{ cm}^{-1}$. Starting from 16.2 GPa, the third lowest-frequency mode (204 cm^{-1}) disappeared and concomitantly a new band on the high-frequency side (309 cm^{-1}) developed, indicating a phase transition. This transition pressure is close to that observed at room temperature (i.e., 17.5 GPa), except that here the transition becomes evident in the external modes instead of internal modes.

C. Synchrotron infrared spectra

We obtained mid- to far-IR spectra for solid SO_2 at high pressures using synchrotron radiation. Figure 5 shows the room-temperature infrared-absorption spectra of SO_2 at $50\text{--}3000\text{ cm}^{-1}$ at selected pressures from 2.2 to 21.3 GPa. As for the Raman spectra, distinct regions are evident: the lattice region up to 400 cm^{-1} , the ν_2 bending region at $553\text{--}596\text{ cm}^{-1}$, ν_1 symmetric stretching at $1153\text{--}1190\text{ cm}^{-1}$, ν_3 asymmetric stretching at $1280\text{--}1356\text{ cm}^{-1}$, and the overtone/combination region at $2467\text{--}2513\text{ cm}^{-1}$.

The spectrum at 2.2 GPa exhibits no lattice features or the ν_2 bending mode; only ν_1 , ν_3 , and a combination mode at 2464 cm^{-1} are observed. This indicates a different phase than seen at higher pressures, consistent with II to III transition¹³ indicated by the previous and current Raman measurements. Starting from 4.3 GPa, two far-IR peaks at 101 and 174 cm^{-1} and the ν_2 bending mode at 559 cm^{-1} become prominent. With increasing pressure, the frequencies of all IR-active bands increase, except for the ν_3 mode, which appears as a blended doublet and is relatively insensitive to pressure. Although the band is significantly broadened by pressure, the separations between the two peaks remain constant over a large pressure region up to 14.9 GPa. On further compression, the low-frequency component has a discernible nega-

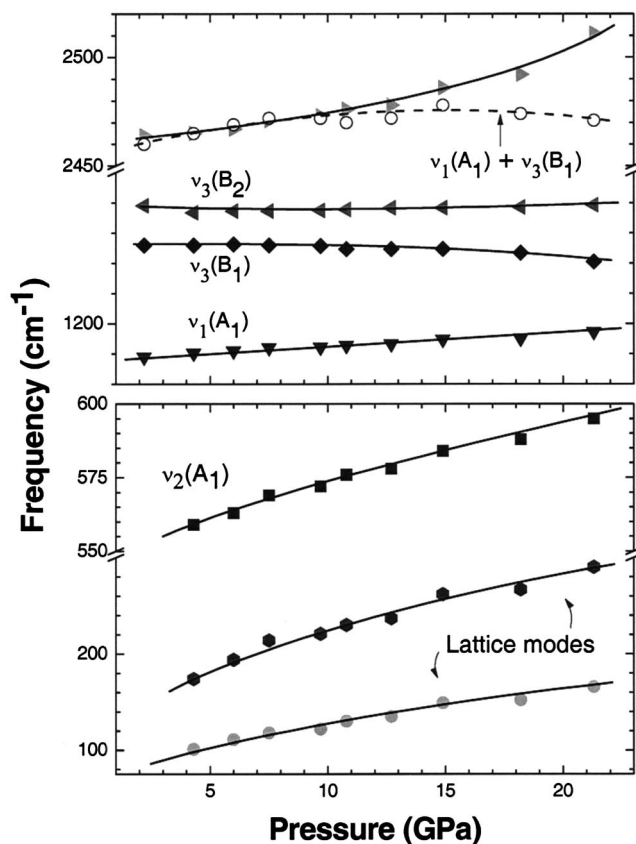


FIG. 6. Pressure dependence of frequencies of IR-active modes of solid SO₂. Different symbols denote different IR peaks.

tive frequency shift, resulting in a larger doublet splitting. Figure 6 summarizes the pressure dependence of the frequencies of all observed IR modes.

In addition to the IR fundamentals, a higher-frequency peak is observed at all pressures. This peak can be assigned as the combination of the ν_1 mode and the low-frequency component of ν_3 . For instance, at 4.3 GPa the sum of 1156 and 1304 cm^{-1} modes is close to the observed peak at 2464 cm^{-1} . As seen in Fig. 6, this assignment fits at pressures below 14.9 GPa, but not above that pressure. This change coincides with the proposed phase transition. (Broadening of the ν_3 mode may also be responsible since the accurate determination of the convoluted peaks is difficult.) Other new IR features are also observed above 14.9 GPa. For instance, the first lattice mode developed an obvious shoulder at lower frequency and the second lattice mode becomes significantly broader and more intense. In addition, the ν_2 bending mode displays a significantly broader profile than at lower pressures. These observations are consistent with a phase transition at 14.5 GPa, slightly lower but close to the pressure where the phase transition was observed in room-temperature Raman spectra.

IV. DISCUSSION

Table I lists the vibrational modes observed in the Raman and infrared spectra of solid SO₂ at high pressures. These observed modes can be assigned consistently based on the previous extensive analysis of ambient pressure struc-

tures of solid SO₂.^{6,7} Sulfur dioxide crystallizes into an orthorhombic cell with four molecules per cell or two molecules per primitive cell.¹⁰ The molecules reside on C_2 sites with the C_2 axis of the molecule (z axis) coincident with the crystallographic c axis. The molecular plane (yz) and the molecular σ_v plane (zx) are approximately parallel to planes which bisect the a and b crystallographic axes. The correlation diagram and the factor group analysis give 15 optical modes which include 6 internal modes of the two SO₂ molecules and 9 external modes involving translational and rotational modes of SO₂ units.⁷

Among the nine lattice modes, three are translational (T) and six are rotational (R); all nine are Raman active and seven are IR active.⁷ In the previous study at ambient pressure and 20 K, all nine Raman modes and six of the IR modes were observed.⁶ These modes occur between 67 and 160 cm^{-1} . Based on the consideration of molecular geometry, molecular interactions as well as comparison between Raman and IR profiles for individual modes, the nine lattice modes are assigned with a pattern of T and R in an intermixed order. However, later Raman measurements on SO₂ at 77 K proposed a modified set of assignments of the lattice modes.⁷ Although fewer bands are observed, the modified assignment complies with the general rule that rotational modes of planar molecules typically have lower frequency and higher intensity than the translational modes, which is also in general accord with lattice dynamics calculations.^{8,20}

To assign the vibrational modes observed for the high-pressure phase, new correlation diagrams are needed for a factor group analysis based on the crystal structures of the new phases. This involves comparison of our Raman and IR data with results obtained at ambient pressure.^{6,7,9} For this purpose, we extrapolated the frequencies of all the observed optical modes to zero pressure. The extrapolated values are given in parentheses in Table I. As can be seen, our extrapolated lattice frequencies do not match those seen at ambient pressure. Low-frequency modes (below 102 cm^{-1}) were seldom resolved in our study, but more modes are observed in the higher-frequency region above 102 cm^{-1} , the rotational mode with the highest frequency at ambient pressure.⁷ Therefore, more Raman- and/or IR-active lattice modes are associated with the high-pressure SO₂ phase. This indicates that there are at least two and probably more SO₂ molecules per primitive cell. Without x-ray diffraction data, we cannot specify symmetries, but can temporarily classify the observed modes based on their frequencies. Tentative assignments of rotational and translational modes of SO₂ are listed in Table I, obtained by comparing our extrapolated values with the previous Raman data.⁷

The observed splittings of fundamentals can be understood as arising from transverse-optical/longitudinal-optical (TO/LO) vibrations.^{6,7} For acentric crystals the TO/LO splittings may be observed in the Raman spectra if the mode is simultaneously IR active.^{21–24} At both room and low temperatures, we observed two components of the ν_1 mode corresponding to the TO and LO vibrations with A_1 symmetry at most pressures (Figs. 1 and 3). The magnitude of the splittings and the intensity of the components are both pressure and temperature dependent. At room temperature and

TABLE I. Vibrational bands observed in solid SO₂ up to 17.5 GPa.

This work		Reference ^a		Assignment ^f
Raman, 75 K ^b	IR, Room T ^c	Raman, 77 K ^d	IR, 77 K ^{d,e}	
		66	67	} R
		69	80	
	111(88)	73	86	
126(104)		99	102.5	
133(110)				} T
148(118)				
164(138)		140	138	
186(155)				
197(159)	194(155)		159	} v ₂
237(199)				
536(530)	563(552)	521.9	522	A ₁
		524.3	ia ^g	A ₂
564(551)		543		A ₁ (LO)
1158(1163)	1164(1148)	1143.8	1144.8	A ₁
		1148.2	ia ^g	A ₂
1178(1177)		1153.8		A ₁ (LO)
1295(1300)	1305(1314)	1310.6	1315.2	B ₁
	1349(1350)	1323.4	1323.2	B ₂
		1337		B ₁ (LO)
		1353		B ₂ (LO)
	2467(2459)			v ₁ (A ₁)+v ₃ (B ₁)

^aFrequencies with different isotopomers SO₂ are not distinguished; see text.

^bFrequencies measured from Raman spectra at 16.2 GPa and 75 K; values extrapolated to ambient pressure are in the parentheses.

^cFrequencies measured from IR spectra at 14.9 GPa and room temperature; values extrapolated to ambient pressure are in parentheses.

^dFrom Ref. 7.

^eFor mid-IR region (>522 cm⁻¹), frequencies are from Ref. 9 which were measured at 77 K and for far-IR region, only 20 K data are available from Ref. 6.

^fR and T denote rotational and translational modes; detailed assignments are omitted due to the unknown structure at high pressure. For the fundamentals, default components are TO unless labeled by LO.

^gia denotes IR inactive.

17.5 GPa, the separation between the v_1 (TO) and v_1 (LO) components increased to 69 cm⁻¹ from 14 cm⁻¹ at 2.2 GPa, giving a slope $d(\Delta v_1)/dP=2.8$ cm⁻¹/GPa. At 75 K at 17.5 GPa the slope is 2.2 cm⁻¹/GPa and $\Delta v_1=42$ cm⁻¹. The magnitude of the separation reflects the extent of intermolecular interactions that the interaction between the neighboring SO₂ molecules is enhanced by pressure. The v_1 (TO) mode at both room temperature and low temperature is more intense than the v_1 (LO) mode but the Raman shift of v_1 (TO) is much less sensitive to pressure than the v_1 (LO) mode. Our extrapolated values at zero pressure of v_1 components, 1163 cm⁻¹(TO) and 1177 cm⁻¹(LO), are higher than the Raman frequencies at ambient pressure, 1143.8 and 1153.8 cm⁻¹. In addition, another previously observed v_1 peak with A₂ symmetry⁷ was not resolved in the present study. However, our IR frequency for the v_1 mode, when extrapolated to zero pressure, agrees with that seen in the previous study at low temperature and ambient pressure.⁶

The TO/LO splitting is also observed for v_2 . At room temperature and below 17.5 GPa, the separation between the TO and LO components of v_2 increased smoothly on compression with $d(\Delta v_2)/dP=1.8$ cm⁻¹/GPa; at 75 K, the TO and LO components evolve nearly the same with pressure,

with $d(\Delta v_2)/dP=0.6$ cm⁻¹/GPa. These values are significantly smaller than those for v_1 . At low temperature, the intensity of the TO component remains nearly constant at all pressures while that for the LO component decrease with pressure and cannot be resolved above 19.2 GPa. At room temperature, although TO is observed at all pressures and evolves smoothly on compression (Fig. 2), its profile changed dramatically above 20.7 GPa [Fig. 1(b)]. As a result, the mode observed at this frequency above 20.7 GPa should not be ascribed to the v_2 (TO) mode (depicted as open squares in Fig. 2 above 20.7 GPa). Furthermore, at 17.5 GPa, the LO mode is replaced by another band with broader profile and high frequency. This feature cannot be explained as the continuation of v_2 (LO) since otherwise there would be an abrupt splitting at this pressure point (Fig. 2), as discussed below. Similar to the v_1 mode, the extrapolated frequencies of the v_2 mode at zero pressure are larger than seen in the spectra at ambient pressure (Table I). The v_2 mode with A₂ symmetry was not detected in the present study. Further, the IR mode has a significantly higher frequency (552 cm⁻¹) than found at ambient pressure.⁹ All these observations are consistent with those for v_1 .

Factor group analysis predicts four Raman bands for the

TABLE II. Pressure and temperature dependence of fundamentals and splittings observed in Raman spectra.

<i>i</i>	This work ^a						References		
	$\left(\frac{dv_i}{dP}\right)_{298\text{ K}}$ (cm ⁻¹ /GPa ^a)	$\left(\frac{dv_i}{dP}\right)_{75\text{ K}}$ (cm ⁻¹ /GPa ^a)	Δv_i , cm ⁻¹ 298 K ^b	Δv_i , cm ⁻¹ 75 K ^b	$\left(\frac{dv_i}{dP}\right)_{298\text{ K}}$ (cm ⁻¹ /GPa)	$\left(\frac{dv_i}{dP}\right)_{75\text{ K}}$ (cm ⁻¹ /GPa)	Δv_i , cm ⁻¹ 77 K ^c	Δv_i , cm ⁻¹ 20 K ^d	Δv_i , cm ⁻¹ Calculated ^e
1	1.2 (3.8)	0.7 (2.9)	8	14	2.8	2.2	10.0	4	8
2	1.9 (3.3)	1.7 (2.0)	15	21	1.8	0.6	21.1	11.5	22
3	-1.9 ...	-0.7	26.4 (29.4) ^g	28	58

^aDue to the dominant intensity of the diamond T_{2g} mode, other components of v_3 are not resolved; splitting data are thus not available for this mode. See text.

^bValues listed are extrapolated to zero pressure.

^cFrom Ref. 7.

^dFrom Ref. 6.

^eCalculated TO/LO splittings derived from an approximate formula and gas phase dipole derivatives. See Refs. 28 and 29.

^fValues pertain to the pressure shift of the TO mode for each fundamental; that for the LO mode is shown in parenthesis.

^gSplitting for B_2 symmetry. See text and Table I.

v_3 asymmetric stretching mode, namely, $B_1(\text{TO})$, $B_2(\text{TO})$, $B_1(\text{LO})$, and $B_2(\text{LO})$. All were observed in the previous studies at ambient pressure and low temperature.^{6,7} Unfortunately, due to the low intensity of this feature and the dominant Raman signal from the T_{2g} mode of the diamond anvils, we observed only one component both at room temperature and 75 K; it is assigned as $B_1(\text{TO})$. By using type-IIa diamond anvils, we were able to observe both IR bands (B_1 and B_2) at all pressures. In fact, these are the strongest internal IR bands. Similar to v_1 and v_2 , the TO/LO splittings should also be observable for this mode by using ¹³C anvils, or by loading isotopically labeled SO₂ in a standard cell to avoid the T_{2g} Raman mode.

The most intriguing high pressure behavior observed for the v_3 asymmetric stretching mode of SO₂ is the softening of the B_1 component. Molecular vibrations typically exhibit positive pressure-induced frequency shifts since chemical bonds tend to stiffen when compressed. Mode softening is therefore often associated with a phase transition at higher pressures.^{19,25,26} In the current case, v_3 (B_1) softens monotonically both in the IR spectra and low-temperature Raman spectra. In contrast, this mode exhibits a “turnaround” pattern at 17.5 GPa in the room-temperature Raman spectra (Fig. 2). Up to 17.5 GPa, the frequency decreases on compression; above that pressure, the frequency increases. This indicates giving a distinct boundary of phase transition. A simple interpretation is that in the lower-pressure phase the v_3 (B_1) mode is soft while in the new higher-pressure phase, this mode becomes “normal.” Although the longitudinal component of v_3 (B_1) is not observable in the Raman spectra, being obscured by the diamond anvil, we can infer the likely behavior of this component. The $v_3(\text{LO})$ frequency probably shifts upwards on compression. That would make the TO/LO splittings consistent with those for v_1 and v_2 on compression, and correspond to enhanced intermolecular interactions as usual. Since the frequency of the diamond T_{2g} Raman mode increases with pressure, the $v_3(\text{LO})$ band would have been observable if it were to shift downwards.

The observation of TO/LO splittings invites theoretical

studies, in particular, of the dependence of splitting magnitude on both pressure and temperature. In Table II we list the dependence of the three fundamentals and their splittings on pressure and temperature. Under different conditions, the splittings vary significantly. For example, Anderson and Campbell⁶ observed Δv_1 , Δv_2 , and Δv_3 values of 4, 11.5, and 28 cm⁻¹, respectively, at 20 K, while those observed by Brooker⁷ are 10.0, 21.1, and 26.4 cm⁻¹ (29.4 cm⁻¹ for LO). Our extrapolated Δv_1 and Δv_2 are 14 and 21 cm⁻¹ at 75 K and 8 and 15 cm⁻¹ at room temperature. These data consistently have $\Delta v_1 < \Delta v_2 < \Delta v_3$ with pressure enhancing all the observed splitting. However, the results from different sources indicate a temperature dependence of the splitting on temperature that needs to be examined theoretically.

In the high-pressure Raman study of solid sulfur dioxide by Brooker,⁷ the complex profiles of all three fundamentals were ascribed to isotopic effects involving either ³⁴S or ¹⁸O or their combinations. Detailed assignment of isotopic SO₂ bands and quantitative analysis of the isotopic shifts in comparison with gas phase Raman spectra were reported.⁷ Isotopic effects were not considered in the work of Swanson *et al.*¹³ In our Raman spectra, no isotopic peaks were resolved. We believe that although at ambient pressure sulfur and oxygen isotopes could contribute to Raman profiles, this is much less likely at high pressure. The natural abundance for ³⁴S vs ³²S is only 4% vs 95% (and $\leq 1\%$ for ³³S and other isotopes); that for ¹⁸O vs ¹⁶O is only 0.2% vs 99.7%. In addition, at high pressure weak peaks may be broadened and possible enhancement of fluorescence could contribute to the lack of clearly resolved isotope features. Also in the DAC, the strong diamond T_{2g} mode may obscure weak peaks in the vicinity. Therefore, considering the large splitting and the strong intensity of the TO/LO components, we deem it appropriate to ignore the isotopic effect in both Tables I and II.

In the low-pressure region below 2.5 GPa, our study is in general accord with previous work.¹³ In that study, a disordered phase (phase II) was reported to exist between 0.3 and 2.5 GPa; this phase is characterized by the broad profile of v_2 and v_1 around 525 and 1140 cm⁻¹. In our spectra

(Fig. 1), the pattern at 1.2 GPa exhibits the characteristics of phase II, while that at 2.2 GPa can be ascribed to phase II-III coexistence. Since pressure calibration was within 0.05 GPa (quasihydrostatic conditions), we conclude that the transition may start at a lower pressure than 2.5 GPa. The transition hysteresis appears larger than the 0.6 GPa previously indicated. The lack of a lattice feature and the broad profile of the ν_2 and ν_1 fundamentals are consistent with a disordered structure (again ν_3 is not observed due to the diamond T_{2g} band). Although such features are also typically associated with a fluid phase, freezing of SO_2 was clearly observed at 0.3 GPa. Unfortunately, the Raman spectra of fluid SO_2 in this lower pressure range have not been reported.¹³ Further studies are needed to clarify the structure of this disordered phase II and its possible relationship to a denser fluid phase.

Our high-pressure Raman spectra, including the lattice modes and fundamentals, are also consistent with the previously observed¹³ phase III, but indicate that this phase extends to 17.5 GPa based on the Raman measurements. Aggregation of SO_2 to form a trimer, $(\text{SO}_2)_3$, was proposed¹³ as the basic structure of this phase III, based on the analogy to the known²⁷ trimeric cluster of $\alpha\text{-SO}_3$. However, the authors assumed a centric space group, even for ambient pressure solid SO_2 , which contradicts orthorhombic with acentric space group determined by single crystal x-ray data.¹⁰ Furthermore, their interpretation of phase III is also inconsistent with later extensive Raman investigation.²⁴ Therefore, although we have observed similar high-pressure behavior of SO_2 , we favor the interpretation indicated by factor group analysis, where the unit cell contains monomeric SO_2 molecules and the splittings are the result of interactions between neighboring molecules in an acentric cell. The additional lattice modes observed in the present study (Table I), in excellent agreement with Swanson *et al.*,¹³ indicate that there are more than two molecules per primitive cell. The information on the unit cell structure and molecular geometry associated with this phase requires diffraction measurements.

Above 17.5 GPa, the major changes in room-temperature Raman spectra are evidence for a new high-pressure phase of sulfur dioxide, designated as phase IV. The appearance of new peaks at 653 cm^{-1} and the doublet around 1244 cm^{-1} suggests the formation of new structures with distinct geometries and chemical bonding rather than rearrangement of weakly interacting SO_2 molecules. The Raman features observed above 17.5 GPa can be rationalized in terms of new bonds between SO_2 units. First, the vibrational frequencies of the clusters should have similar modes possessed by other sulfur compounds where sulfur is multiply coordinated by oxygen, such as sulfones, sulfoxides, or sulfate compounds. These compounds have SO_2 -, SO_3 -, or SO_4 structures with vibrational frequencies at 500–610 cm^{-1} corresponding to SO_2 scissor motion, at 1120–1230- cm^{-1} asymmetric stretching, or 565–675 cm^{-1} for SO_4 bending modes. The frequencies for the new Raman modes observed for phase IV, if extrapolated to zero pressures, are close to those associated with these sulfur compounds. Second, although these modes (650 and 1244 cm^{-1}) are observed at frequencies where the $\nu_2(\text{LO})$ and $\nu_1(\text{LO})$ modes occur, the very different band profile (Fig. 1) and the prominent discon-

tinuity of the Raman shifts with pressure (Fig. 2) suggest that they are new bands associated with a new structure. That the TO/LO splittings are no longer observed above 17.5 GPa is consistent with a structure (in strong contrast to phase III), wherein three or more monomeric SO_2 molecules crystallize in an acentric cell. Third, the turnaround behavior of the ν_3 mode of SO_2 (Fig. 2) is further evidence for the formation of a new structure of SO_2 . In phase III, the ν_3 mode associated with the asymmetric stretch of SO_2 molecules (near 1300 cm^{-1}) is a soft mode indicating that a transition will occur at higher pressures. Lastly, further compression of solid SO_2 above 17.5 GPa appears to complete a phase transition. The new features at 653 and 1244 cm^{-1} that arise at 17.5 GPa continue to develop and at 25.6 GPa become the dominant bands. Low-temperature Raman spectra (Fig. 3), however, do not reveal the same features observed at room temperature. Only one new band is observed below ν_1 starting at 9.2 GPa. We conclude that in the pressure range of our study, SO_2 remains an ordered structure, possibly similar to the room-temperature structure. The observation of soft mode at 1151 cm^{-1} (Fig. 4) indicates that a phase transition will occur at higher pressures.

V. CONCLUSIONS

We present a systematic study of the vibrational spectra of SO_2 at high pressure. Splittings are observed for the ν_1 and ν_2 fundamentals that are ascribed to transverse-optical/longitudinal-optical splittings. These are consistent with the crystal structure previously determined by single-crystal x-ray diffraction. Analysis of the splittings indicates that interactions between neighboring SO_2 molecules are enhanced by pressure, while the dependence of the splittings on temperature remains unclear. Our study finds evidence for two phases (II and III) of solid SO_2 , consistent with previous reports, and it extends the range of stability of phase III up to 17.5 GPa. We suggest that phase III has an acentric cell similar to that at ambient pressure but with three or more SO_2 molecules per cell. This interpretation differs from the previously proposed structure involving trimeric clusters. Prominent new features observed above 17.5 GPa in room-temperature Raman spectra and a turnaround of the ν_3 asymmetric stretching band suggest a transition to a new phase (IV). This possibly involves SO_2 clusters with the sulfur atom multiply coordinated by oxygen atoms. Distinct behavior of the evolution of the Raman modes on compression at 75 K and at room temperature further suggests that the transition to phase IV at low temperatures requires higher pressure. Vibrational absorption spectra in both the far- and mid-IR range provide information about phase transitions consistent with that from Raman spectra. X-ray diffraction studies in progress should elucidate high-pressure structures of sulfur dioxide.

ACKNOWLEDGMENTS

This work was supported by Lawrence Livermore National Laboratory (Subcontract No. B525927 to Harvard University) and NSF (Grant No. DMR-0205899). IR measurements were performed at the U2A beamline at NSLS of

BNL (DOE Contract No. DE-AC02-98CH10886). The U2A beamline is supported by COMPRES, the Consortium for Materials Properties Research in Earth Sciences under NSF Cooperative Agreement Grant No. EAR01-35554, and the U.S. Department of Energy (DOE), (CDAC, Contract No. DE-FC03-03N00144).

- ¹G. J. Kubas, *Acc. Chem. Res.* **27**, 183 (1994).
²A. Anderson and S. H. Walmsley, *Mol. Phys.* **10**, 391 (1966).
³A. Anderson and R. Savoie, *Can. J. Chem.* **43**, 2271 (1965).
⁴P. A. Giguere and M. Falk, *Can. J. Chem.* **34**, 1823 (1956).
⁵R. N. Wiener and E. R. Nixon, *J. Chem. Phys.* **25**, 175 (1956).
⁶A. Anderson and M. C. W. Campbell, *J. Chem. Phys.* **67**, 4300 (1977).
⁷M. H. Brooker, *J. Mol. Struct.* **112**, 221 (1983).
⁸P. Procacci, A. Tafi, L. Angeloni, R. Righini, and P. R. Salvi, *Chem. Phys.* **154**, 331 (1991).
⁹A. Barbe, A. Delahaigue, and P. Jouve, *Spectrochim. Acta, Part A* **27**, 1439 (1971).
¹⁰B. Post, R. S. Schwartz, and I. Fankuchen, *Acta Crystallogr.* **5**, 372 (1952).
¹¹R. J. Hemley, *Annu. Rev. Phys. Chem.* **51**, 763 (2000).
¹²R. J. Hemley and H. K. Mao, in *High Pressure Phenomena*, edited by R. J. Hemley *et al.* (IOS, Amsterdam, 2002), p. 3.
¹³B. I. Swanson, L. M. Babcock, D. Schiferl, D. C. Moody, R. L. Mills, and R. R. Ryan, *Chem. Phys. Lett.* **91**, 393 (1982).
¹⁴Y. Song, R. J. Hemley, Z. Liu, M. Somayazulu, H. K. Mao, and D. R. Herschbach, *J. Chem. Phys.* **119**, 2232 (2003).
¹⁵Y. Song, M. Somayazulu, H. K. Mao, R. J. Hemley, and D. R. Herschbach, *J. Chem. Phys.* **118**, 8350 (2003).
¹⁶Y. Song, R. J. Hemley, H. K. Mao, Z. Liu, and D. R. Herschbach, *Chem. Phys. Lett.* **382**, 686 (2003).
¹⁷H. K. Mao, J. Xu, and P. M. Bell, *J. Geophys. Res.* **91**, 4673 (1986).
¹⁸A. F. Goncharov, V. V. Struzhkin, R. J. Hemley, H. K. Mao, and Z. Liu, in *Science and Technology of High Pressure*, edited by M. H. Manghnani, W. Nellis, and M. Nicol (Universities Press, Hyderabad, India, 2000), p. 90.
¹⁹R. C. Hanson, T. A. Fjeldly, and H. D. Hochheimer, *Phys. Status Solidi B* **70**, 567 (1975).
²⁰A. Rostogi, A. Anderson, and J. W. Leech, *Can. J. Phys.* **57**, 2120 (1979).
²¹J. C. Decius and R. M. Hexter, *Molecular Vibrations in Crystals* (McGraw-Hill, New York, 1977).
²²C. K. Asawa and M. K. Barnoski, *Phys. Rev. B* **2**, 205 (1970).
²³C. M. Hartwig, E. Wiener-Avneer, and S. P. S. Porto, *Phys. Rev. B* **5**, 79 (1972).
²⁴M. H. Brooker and D. E. Irish, *Can. J. Chem.* **49**, 1289 (1971).
²⁵S. S. Mitra, O. Brafman, W. B. Daniels, and R. K. Crawford, *Phys. Rev.* **186**, 942 (1969).
²⁶Y. Ebisuzaki and M. Nicol, *J. Phys. Chem.* **33**, 763 (1971).
²⁷R. Westrik and C. H. MacGillavry, *Acta Crystallogr.* **7**, 764 (1954).
²⁸C. Haas and D. F. Hornig, *J. Chem. Phys.* **26**, 707 (1957).
²⁹J. E. Mayhoo, *Can. J. Phys.* **35**, 954 (1957).